COMPARISON OF ANALYTICAL AND EXPERIMENTAL RIB STIFFENER MODIFICATIONS TO A STRUCTURE

Peter Wallack, Paul Skoog and Mark Richardson
Structural Measurement Systems, Inc.
San Jose, California
United States

ABSTRACT

One of the most common ways of adding stiffness to localized areas of a structure is through the use of rib stiffeners. Figure 1 shows a rib stiffener attached to a plate structure. Rib stiffeners are usually attached to the surface of an existing structure by welding, gluing or bolting. Alternatively, they can be cast or molded onto the surface of the structure if the structure is formed by a casting or molding process.

Rib stiffeners are a common means of increasing structural stiffness and can be modeled quickly and simply with the Structural Dynamics Modification (SDM) technique. The main advantage of SDM over Finite Element Analysis (FEA), or prototype fabrication and testing, is its speed. Hence, SDM allows a designer to explore a larger number of design modifications without having to fabricate and retest each one, or without having to build and analyze a variety of different finite element models.

The most effective use of SDM, however, is with the combined use of modal testing and FEA. A finite element analysis and a modal test should be performed on the unmodified structure first. This is done to confirm the validity of the finite element model using the modal test data. SDM can then be more effectively applied to the larger data base of finite element modes.

In this paper, the validity and accuracy of the SDM approach to modeling rib stiffeners is investigated by comparing SDM-generated results with those of an FEA and with modal test results.

First, the modal parameters of a plate structure are generated from a finite element model and are compared to the parameters obtained from a modal test. Then, the modes of the structure are compared after a rib stiffener modification has been modeled using SDM and FEA, and these results are compared with test results taken from the real structure with the rib stiffener attached to it.

INTRODUCTION

In many structures, we would like to add stiffness to a surface to reduce vibration levels. This type of modification should produce restoring (stiffness) forces only when local bending occurs on the surface.

A rib stiffener can be modeled by making additions to the stiffness matrix of the differential equations of motion for the structure. Some addition to the mass matrix should also be made to account for the added mass of the stiffener, but the primary effect is due to the added stiffness.

The equations of motion can be expressed as:

$$\left[M + \Delta M\right]\left\{\ddot{x}(t)\right\} + \left[C\right]\left\{\dot{x}(t)\right\} + \left[K + \Delta K\right]\left\{x(t)\right\} = \left\{f(t)\right\} \quad (1)$$

where:

$\left[\Delta M\right]$ = Addition of the Rib Mass

$\left[\Delta K\right]$ = Addition of the Rib Stiffness

The SDM method is a convenient and efficient means of modeling these required stiffness and mass additions to a structure. SDM requires only the parameters of the "dynamically significant" modes of the unmodified structure and yields the frequency, damping and mode shapes of the modified structure with the rib stiffener attached. This gives an immediate indication of the effect of the rib stiffener upon the modes of vibration of the structure.

In general, the "dynamically significant" modes are those that contribute significantly to the overall dynamics of the structure at the modification points. This can be verified by synthesizing FRFs at and/or between the modification points using the modal data, and comparing the synthesized FRFs with actual FRF measurements.

The SDM method [1] gains some of its computational efficiency by allowing only a single scalar stiffness element

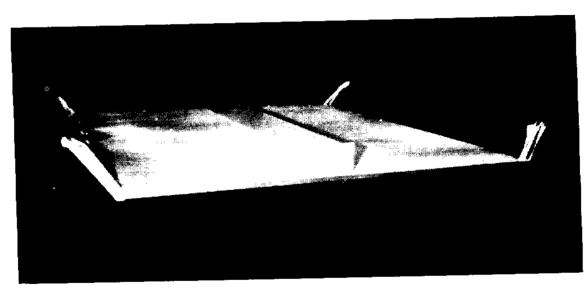

Figure I. Plate with a Rib Stiffener

(or a point mass) to be added with each new eigenvalue solution. The rib stiffener modification requires several stiffness and mass additions, however, and these must be added in a serial manner with SDM.

More recently, the S^2DM method (Simultaneous SDM) [4] has been introduced which allows all of the required modifications to be implemented simultaneously in one eigenvalue solution. Hence, S^2DM provides faster and more accurate solutions to rib stiffener modification problems than the more traditional SDM method.

BACKGROUND THEORY

A rib stiffener can be modeled using an idealized three-point beam, as shown in Figure 2. This three-degree-of-freedom (DOF) beam element is well suited for simulating the effects of a rib stiffener since it will add local bending stiffness to a structure without affecting its rigid body motion.

The force-displacement relationship of the beam element is derived by using the unit-displacement method, as shown in Figure 2. This method involves subjecting the beam to a unit deflection at one DOF and determining the restraining forces needed at the other two DOFs in order to maintain equalibrium. These forces are directly related to the stiffness elements in the forced-displacement relationship for the beam.

The force-displacement relationship can be expressed as:

$$\begin{Bmatrix} F_1 \\ F_2 \\ F_3 \end{Bmatrix} = \begin{bmatrix} k_{11} & k_{12} & k_{13} \\ k_{21} & k_{22} & k_{23} \\ k_{31} & k_{32} & k_{33} \end{bmatrix} \begin{Bmatrix} y_1 \\ y_2 \\ y_3 \end{Bmatrix} \tag{2}$$

Applying a unit deflection at point 1:

$$y_1 = 1,\ y_2 = 0,\ y_3 = 0$$

and calculating the resulting forces at points 1, 2 and 3 gives:

$$\begin{aligned} F_1 &= k_{11}\ y_1 = k_{11} \\ F_2 &= k_{12}\ y_1 = k_{12} \\ F_3 &= k_{13}\ y_1 = k_{13} \end{aligned} \tag{3}$$

Using singularity functions, the force-displacement relationship for the beam can be expressed as:

$$F(x) = y(x) \frac{3EI}{x^3 - L\langle x-a \rangle^3 / 2b - \left(2ab + 3a^2\right) x/2 + a^2 L} \tag{4}$$

Imposing the condition:

$$x = 0, \quad y(0) = y_1 = 1$$

in equation (4) gives:

$$F_1 = 3EI/a^2L = k_{11} \tag{5}$$

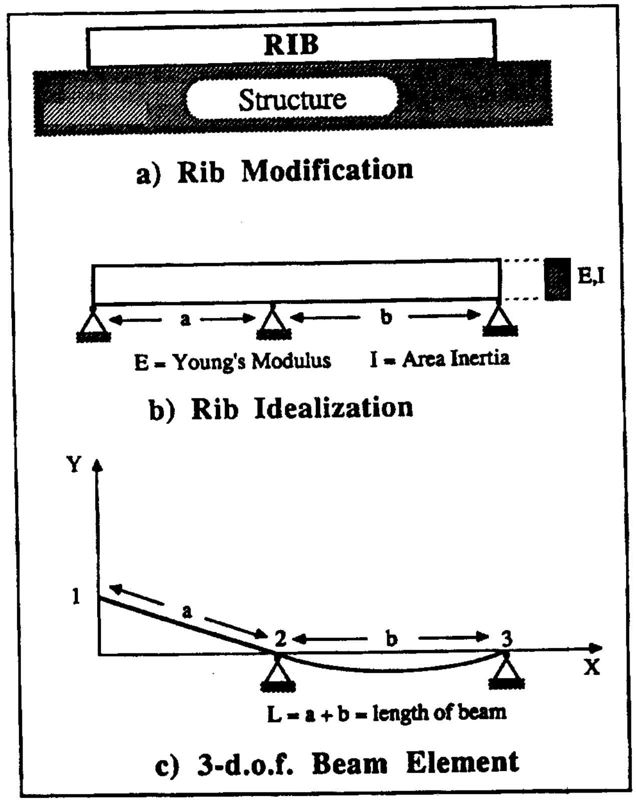

Figure 2. Rib Modification Rib Idealization and Three-DOF Beam Element

Drawing a free-body diagram of the beam and using the value of F_1 in expression (5), the values of F_2 and F_3 are determined as the following:

$$\begin{aligned} F_2 &= -3EI/a^2b = k_{21} \\ F_3 &= 3EI/abL = k_{31} \end{aligned} \tag{6}$$

The rest of the stiffness elements can be determined in a similar manner. The complete force-displacement relationship for the beam therefore becomes:

$$\begin{Bmatrix} F_1 \\ F_2 \\ F_3 \end{Bmatrix} = 3EI \begin{bmatrix} 1/a^2L & & \text{SYM} \\ -1/a^2b & \text{L}/a^2b^2 & \\ 1/abL & -1/ab^2 & 1/b^2L \end{bmatrix} \begin{Bmatrix} y_1 \\ y_2 \\ y_3 \end{Bmatrix} \tag{7}$$

Hence, the stiffness matrix for the three-DOF beam is:

$$[\Delta K]_b = 3EI \begin{bmatrix} 1/a^2L & & \text{SYM} \\ -1/a^2b & \text{L}/a^2b^2 & \\ 1/abL & -1/ab^2 & 1/b^2L \end{bmatrix} \begin{Bmatrix} y_1 \\ y_2 \\ y_3 \end{Bmatrix} \tag{8}$$

Notice that the stiffness is a function of the beam length (L), the spacing between attachment points (a and b), the modulus of elasticity (E), and cross-sectional moment of inertia (l).

This stiffness matrix can also be expressed as the sum of three stiffness matrices, each corresponding to a single scalar stiffness (linear spring) modification:

$$[\Delta K]_b = [\Delta K]_1 + [\Delta K]_2 + [\Delta K]_3 \qquad (9)$$

where:

$$[\Delta K]_1 = \left(3EI/a^2b\right)\begin{bmatrix} 1 & -1 & 0 \\ -1 & 1 & 0 \\ 0 & 0 & 0 \end{bmatrix} \qquad (10)$$

$$[\Delta K]_2 = \left(3EI/ab^2\right)\begin{bmatrix} 0 & 0 & 0 \\ 0 & 1 & -1 \\ 0 & -1 & 1 \end{bmatrix} \qquad (11)$$

$$[\Delta K]_3 = \left(-3EI/abL\right)\begin{bmatrix} 1 & 0 & -1 \\ 0 & 0 & 0 \\ -1 & 0 & 1 \end{bmatrix} \qquad (12)$$

These stiffnesses are now in terms of basic SDM scalar stiffness modifications. To model the attachment of a rib stiffener to the surface of a structure at points 1, 2 and 3 in the Y-direction, the following SDM commands would be used:

STIFFMOD $\left(3EI/a^2b\right)$, 1Y, 2Y
STIFFMOD $\left(3EI/ab^2\right)$, 2Y, 3Y
STIFFMOD $\left(-3EI/abL\right)$, 1Y, 3Y

Notice that the first two modifications add stiffness, while the third modification removes a lesser amount than either of the first two. After each command is entered, a new set of modal data is determined by SDM which reflects the effect of the scalar modification. (In order to use SDM, the attachment points must be where mode shape data is defined).

Using S^2DM, these three modifications would be entered into a table, and one solution that reflects the effect of the entire rib stiffener would be computed.

The mass of the rib stiffener must also be added to the structure to correctly model the attachment of the stiffener. This is very simply done by distributing the mass proportionally among the three attachment points, as shown in Figure 3.

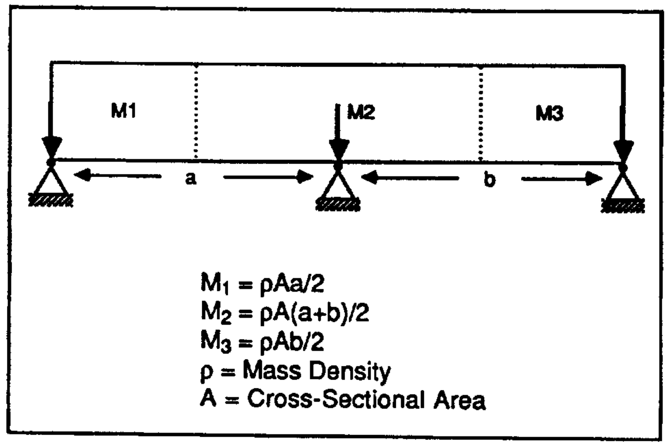

Figure 3. Mass Distribution

This would yield the following mass matrix addition:

$$[\Delta M] = rA\begin{bmatrix} a/2 & 0 & 0 \\ 0 & (a+b)/2 & 0 \\ 0 & 0 & b/2 \end{bmatrix} \qquad (13)$$

To complete the modeling of the rib stiffener, these three mass modifications would be added to the structure with three point mass additions using SDM as follows:

MASSMOD $\left(rAa/2\right)$, 1Y
MASSMOD $\left(rA(a+b)/2\right)$, 2Y
MASSMOD $\left(rAa/2\right)$, 3Y

Again, S^2DM can apply all six modifications (three mass and three stiffness) to the structure in one eigen-solution, thus increasing the speed and accuracy of this technique.

RIB STIFFENERS WITH MORE THAN THREE DOFS

In many practical applications, we would like to model the attachment of rib stiffeners at more than three points on a structure. One way of doing this is to simply string together several three-DOF rib stiffeners end-to-end in a line across the structure, attaching them at each point where modal data exists, as shown in Figure 4. However this method doesn't apply any moment to the structure at the end-points of each three-DOF beam and, therefore, won't correctly model a real rib.

The method shown in Figure 5, i.e., layering the three DOF beams in a brick-wall manner, more correctly models a multi-point stiffener, but requires a special beam element at the ends of the rib.

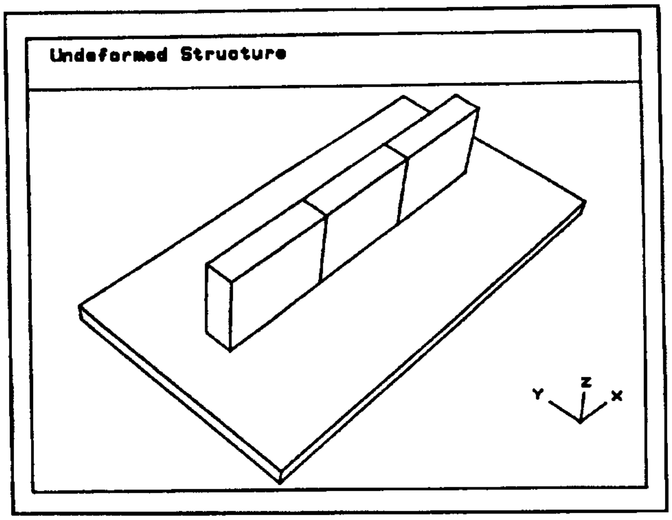

Figure 4. End-to-End Beam Elements

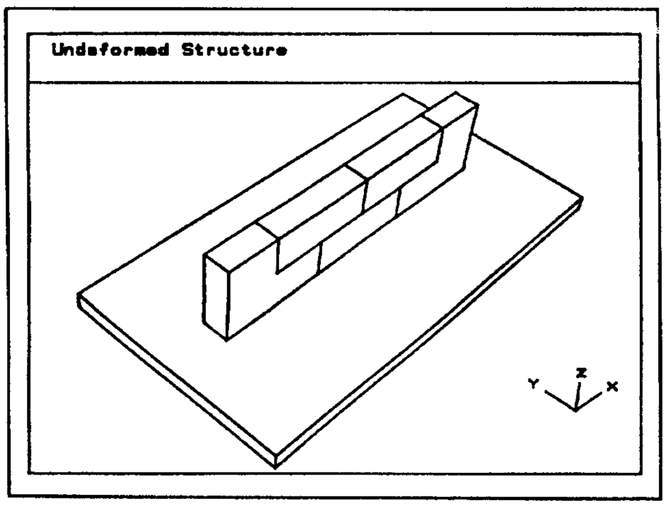

Figure 5. Layered Beam Elements

In [2], it was proposed that the three-DOF beams be stacked side-by-side, as shown in Figure 6. This method also requires the use of a special beam element at the ends of the rib, though.

In this paper, two new methods of using the three-DOF beam element to model multi-DOF ribs are examined. Both are simpler to implement than the previous methods, and are depicted in Figures 7 and 8.

MAXIMUM OVERLAPPING STIFFNESS (MOS)

This method places the three-DOF beam elements on the structure so that they overlap between each pair of attachment points. This case is different than those presented in Figures 5 and 6 in that the entire cross-sectional area of the rib is used instead of half the area, hence the cross sectional inertia (1) is different. For example, the inertias of the side-by-side beams used in Figure 6 would be half the inertia used for the MOS model.

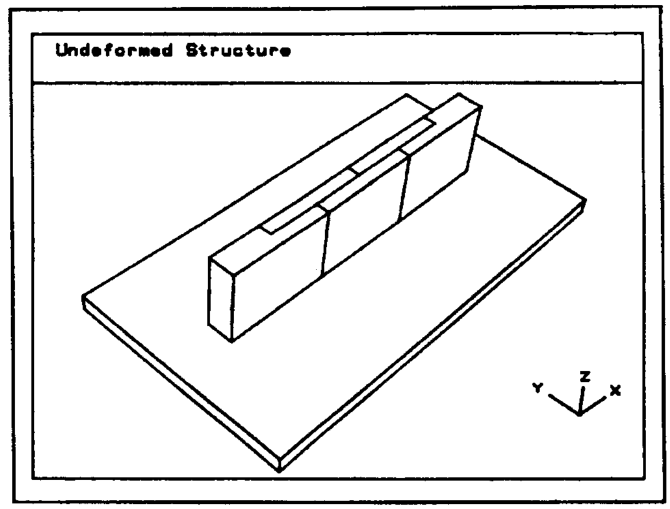

Figure 6. Side-by-Side Beam Elements

In this method, the *maximum* of the stiffness created by each three-DOF beam is used between each pair of attachment points where two beams overlap. In Figure 7, only two beams are needed to model the rib, and they overlap between points 2 and 3.

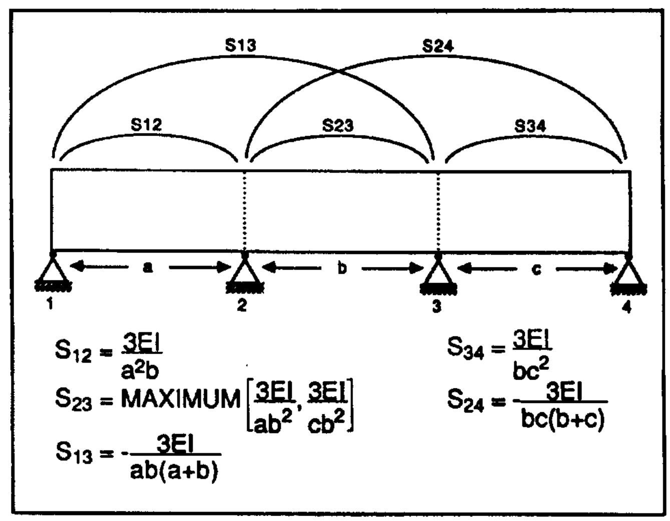

Figure 7. Maximum Overlapping Stiffness

SUMMATION OF OVERLAPPING STIFFNESSES (SOS)

This model is similar to the MOS model and even simpler in that the stiffnesses caused by the overlapping beams are merely summed together. In the example shown in Figure 8, the beams overlap between points 2 and 3 and, therefore, the stiffness between those two points is the sum of the stiffnesses caused by the two beam elements.

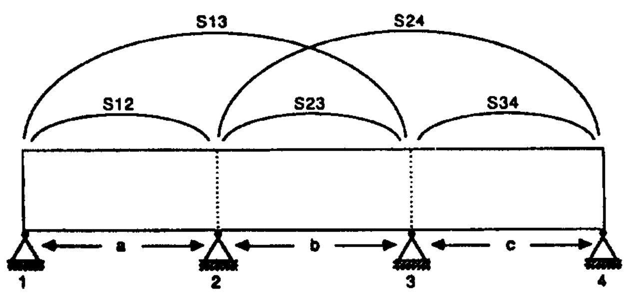

$$S_{12} = \frac{3EI}{a^2 b} \qquad S_{34} = \frac{3EI}{bc^2}$$

$$S_{23} = \frac{3EI}{ab^2} + \frac{3EI}{b^2 c} \qquad S_{24} = -\frac{3EI}{bc(b+c)}$$

$$S_{13} = -\frac{3EI}{ab(a+b)}$$

Figure 8. Summation of Overlapping Stiffnesses

THE FINITE ELEMENT ANALYSIS (FEA) MODELS

Two FEA models of the plate were developed; one for the plate without the rib and one for the plate with the rib. The latter model was an extension of the former. The actual structure is a .52 x .419 x .007 m aluminum plate. A 6 x 5 point grid dividing the plate into 20 equal sized rectangles was overlaid on the plate and 4.76 mm holes were drilled at all 30 points on the grid. This grid defined the 20 elements used in the FEA as well as the test points for the modal test. By using the same points for both the FEA model and the modal test, we were assured of the correct correlation of results in the later analysis.

The rib stiffener was an aluminum bar measuring .52 x .032 x .009 m. It was secured to the plate along the lengthwise centerline with six screws.

The FEA plate model was composed of 20 shell bending elements. Standard material properties were assigned from a general machine design handbook. Since there were 30 drill holes in the structure, point masses were subtracted from the model at the node points. (It was found that subtracting the inertia of the missing drill hole material from the model had little effect.) The rib was modeled using five shell bending elements.

The FEA involved analyzing the structure in a free-free condition extracting the first eight dynamic modes of each model. The model for the plate contained 180 DOFs, while the model for the plate and rib contained 216 DOFs. Each node used six DOFs, though only the Z direction DOFs were used in the final SDM and Modal Assurance Criterion (MAC) analyses and mode shape comparisons. It was found that the FEA model was very sensitive to plate thickness and point mass removal. *Changing the plate thickness as little as .254 mm could result in 10 Hz. shifts in the fundamental frequency. As* a result, accurate measurements of the physical model were necessary for frequency correlation with the FEA models.

The FEDESK Desktop Finite Element Analysis program was used for all FEA. The FEA mode shapes for both the plate and ribbed-plate models were transferred to the SMS MODAL 3.0 SE Modal Analysis System via SASTRAN. SASTRAN is a FEDESK-to-MODAL 3.0 SE database translator.

MODAL TEST OF PLATE

A test plate was fabricated from aluminum and drilled with 30 equally spaced holes to allow the rib to be attached to the plate at several locations. The specimen was mounted in a test fixture by hanging it from soft supports (rubber bands) at its corners. The two modal surveys, (with and without the rib), were conducted using a calibrated impact hammer and response accelerometer, FFT analyzer and the SMS MODAL 3.0 SE System. A global curve fitter was used to extract the modal parameters from FRF measurements made with the analyzer. Thirty measurements were made per survey, impacting only in the direction normal to the surface of the plate.

COMPARISON OF FEA AND TEST RESULTS

Figure 9 shows the FEA and experimental modal frequencies for the plate without rib. Modal damping is also included with the experimental data since it is always present and measurable in test data. Notice, however, that the damping is very light, thus making the normal mode (zero damped) data from the FEA a good approximation of the real world.

Figure 9 also contains the MAC values [5] for the FEA and experimental mode shapes. MAC values close to one (1) along the diagonal indicate that the two sets of mode shapes are nearly identical to one another.

Figure 10 shows the mode shapes of the first eight modes of the plate.

RIB STIFFENER MODIFICATIONS

The rib stiffener modification to the plate was performed in six different ways and the results are compared here.

Modal Frequency and Damping

	FEA Modes		Exp. Modes	
Mode	Freq (Hz)	Damp (%)	Freq (Hz)	Damp (%)
1	98.745	0.000	98.338	.179
2	120.698	0.000	125.449	.061
3	192.060	0.000	206.210	.050
4	222.754	0.000	235.582	.113
5	247.345	0.000	276.301	.041
6	334.002	0.000	365.893	.073
7	388.714	0.000	459.370	.094
8	406. 227	0.000	468.273	.101

Modal assurance Criterion (MAC)

	FEA Modes							
Exp. Modes	1	2	3	4	5	6	7	8
1	1.00	0.00	0.00	0.00	0.00	0.00	.04	0.00
2	0.00	.99	.01	0.00	0.00	0.00	0.00	.04
3	0.00	0.00	.99	0.00	0.00	0.00	0.00	.06
4	0.00	0.00	0.00	.99	0.00	0.00	0.00	0.00
5	0.00	0.00	0.00	0.00	.99	.04	0.00	0.00
6	0.00	0.00	0.00	0.00	0.00	.97	0.00	0.00
7	.07	0.00	0.00	.01	0.00	0.00	.94	.04
8	0.00	.03	.08	0.00	0.00	0.00	.04	.95

Figure 9. FEA Versus Experimental Modes for Plate Without Rib

The six different cases were:

1. Modal test of the plate and rib.
2. FEA of the plate and rib.
3. SDM using MOS rib model and FEA data.
4. SDM using SOS rib model and FEA data.
5. SDM using MOS rib model and experimental data.
6. SDM using SOS rib model and experimental data.

S^2DM was run on both FEA and experimental modal data. The following values were used to model the rib stiffener:

- Young's Modulus: 71,000,000,000 Pa
- Base of rib: 9.5 mm
- Height of rib: 31.75 mm
- Mass distribution: .045 kg at ends of rib
  .091 kg at internal points of rib

S^2DM solutions typically took about 20 seconds on a desktop computer to model the attachment of the rib, using eight modes of vibration.

The modal frequencies for these six cases are compared in Figure 11. The mode shapes for the plate and rib are shown in Figure 12 and the MAC values for cases 2 through 6 versus the experimental data (case 1) are given in Figure 13.

CONCLUSIONS

The data in Figure 9 shows that the FEA model of the plate without rib tended to give slightly lower modal frequencies than the test data as the modes increased in frequency. The FEA mode shapes, however, were virtually identical to the test mode shapes, as indicated by the MAC values in Figure 9.

Since the FEA and experimental modal frequencies were different, we used both data sets with SDM to see if the difference in frequencies alone would improve the accuracy of the SDM results.

The plate with rib frequencies in Figure 11 seem to indicate that the SOS rib model gave more accurate results than the MOS model. More specifically, the SOS frequencies matched the experimental results better than the MOS frequencies. However, an examination of the MAC values shows that several of the mode shapes are quite different in the SDM results from the experimental results.

One factor which could contribute significantly and which was pointed out in reference [2], is the influence of rotational DOFs. A clear advantage of using the FEA data is that it contains rotational DOFs, whereas the test data does not. Although they were not considered here, perhaps stiffening the rotational DOFs at the rib attachment points would have improved the SDM results somewhat.

	Exp.	FEA
Mode	Freq (Hz)	Freq (Hz)
1	106.687	106.759
2	190.636	177.859
3	247.650	233.181
4	259.222	233.920
5	261.955	239.958
6	470.489	397.327
7	494.810	414.929

	From Exp.		From FEA	
	MOS	SOS	MOS	SOS
Mode	Freq (Hz)	Freq (Hz)	Freq (Hz)	Freq (Hz)
1	97.905	98.687	98.745	98.745
2	153.418	191.847	117.632	174.271
3	195.925	217.899	179.631	208.394
4	235.546	236.210	222.754	222.754
5	374.892	258.015	367.838	235.748
6	459.119	459.225	388.720	388.716
7	520.118	520.118	455.778	437.944

Figure 11. Modal Frequencies for Plate With Rib

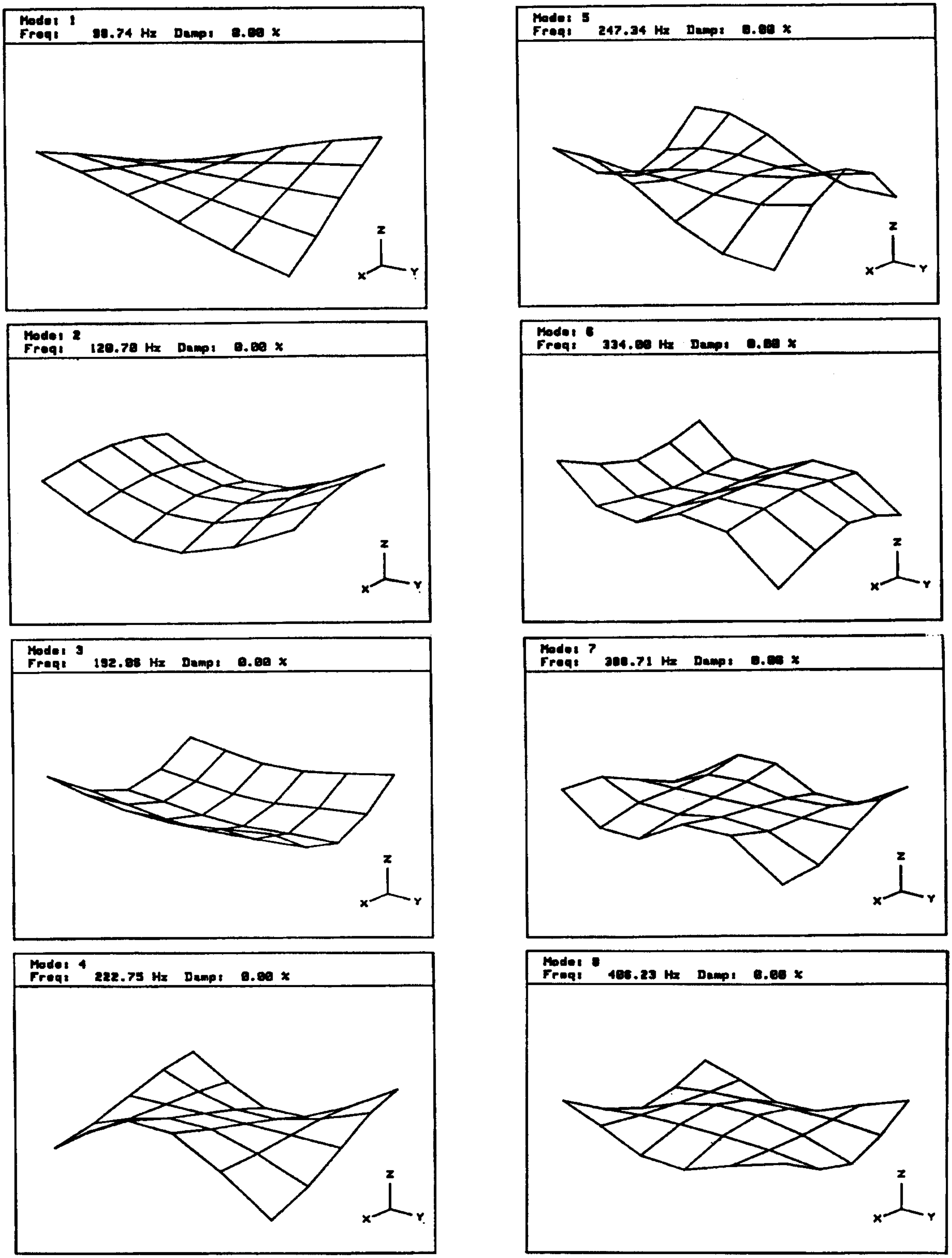

Figure 10. Modes Shapes of Plate Without Rib

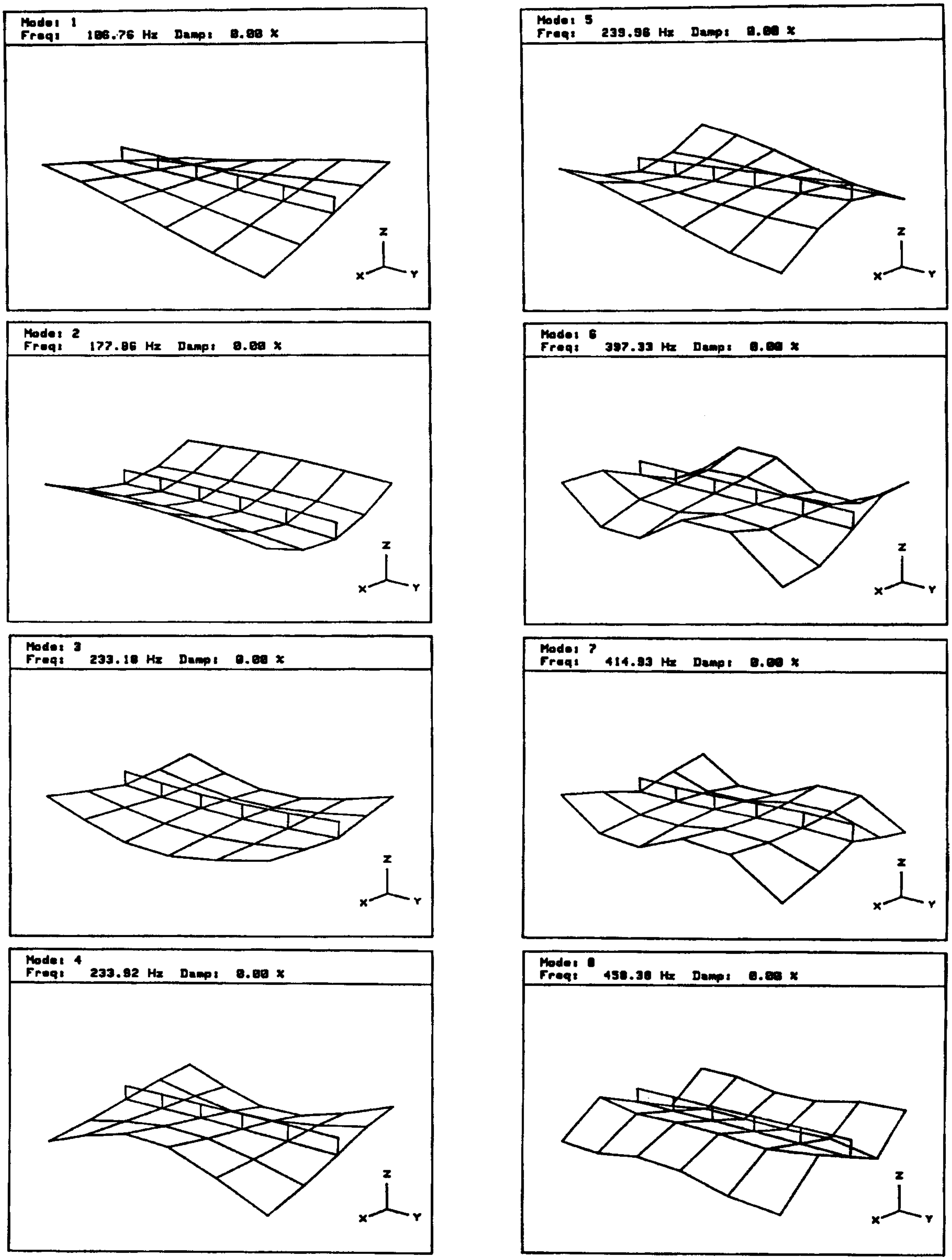

Figure 12. Mode Shapes for Plate With Rib

The MAC values in Figure 11 indicate that the FEA mode shapes didn't match the experimental shapes well either.

Figure 14 shows the MAC values for the FEA modes of the plate and rib with the S^2DM and SOS model mode shapes. This indicates very good agreement between these two different analytical methods, even though there are still discrepancies with the test results.

		Experimental Modes						
	Mode	1	2	3	4	5	6	7
FEA	1	.98	0.00	0.00	0.00	.01	.07	0.00
	2	0.00	.97	0.00	0.00	0.00	0.00	0.00
	3	0.00	.02	.04	.41	.53	0.00	.01
	4	0.00	0.00	.92	.03	.03	.01	0.00
	5	0.00	0.00	.01	.54	.38	0.00	.03
	6	.05	0.00	0.00	0.00	0.00	.96	.01
	7	0.00	0.00	0.00	.02	.01	0.00	.94

		Experimental Modes						
	Mode	1	2	3	4	5	6	7
MOS From FEA	1	.98	0.00	0.00	0.00	.01	.07	0.00
	2	0.00	0.00	.01	.52	.35	0.00	.10
	3	0.00	.93	0.00	.01	.02	0.00	.01
	4	0.00	0.00	.92	.03	.03	.01	0.00
	5	0.00	.01	.03	.54	.32	0.00	.01
	6	.04	0.00	0.00	0.00	0.00	.95	.02
	7	0.00	0.00	0.00	0.00	.01	0.00	.77

		Experimental Modes						
	Mode	1	2	3	4	5	6	7
SOS From FEA	1	.98	0.00	0.00	0.00	.01	.07	0.00
	2	0.00	.86	0.00	.05	.04	0.00	0.00
	3	0.00	.12	.04	.36	.47	0.00	.01
	4	0.00	0.00	.92	.03	.03	.01	0.00
	5	0.00	0.00	.01	.53	.37	0.00	.03
	6	.04	0.00	0.00	0.00	0.00	.95	.02
	7	0.00	.01	.02	.11	.15	0.00	0.00

		Experimental Modes						
	Mode	1	2	3	4	5	6	7
MOS From Exp.	1	.97	0.00	0.00	.01	.01	.07	0.00
	2	.04	0.00	.01	.47	.39	0.00	.07
	3	0.00	.94	0.00	0.00	.03	0.00	.01
	4	0.00	0.00	.92	.03	.03	.01	0.00
	5	0.00	.01	.02	.26	.42	0.00	0.00
	6	.07	0.00	0.00	0.00	.01	.97	0.00
	7	.01	0.00	.01	0.00	.01	.01	.78

		Experimental Modes						
	Mode	1	2	3	4	5	6	7
SOS From Exp.	1	.98	0.00	0.00	0.00	.01	.07	0.00
	2	0.00	.83	.01	.05	.05	0.00	0.00
	3	0.00	.06	.12	.34	.48	0.00	.01
	4	0.00	0.00	.82	.07	.06	.01	0.00
	5	.01	0.00	0.00	.50	.42	0.00	.01
	6	.07	0.00	0.00	0.00	0.00	.98	0.00
	7	0.00	0.00	.01	.11	.20	0.00	0.00

Figure 13. MAC Values for Experimental Versus Analytical Mode Shapes

		FEA Modes						
	Mode	1	2	3	4	5	6	7
SOS From FEA	1	1.00	0.00	0.00	0.00	0.00	.05	0.00
	2	0.00	.88	.04	0.00	0.00	0.00	0.00
	3	0.00	.13	.93	0.00	0.00	0.00	0.00
	4	0.00	0.00	0.00	1.00	0.00	0.00	0.00
	5	0.00	0.00	0.00	0.00	.99	0.00	.05
	6	.04	0.00	0.00	0.00	0.00	1.00	0.00
	7	0.00	.01	.25	0.00	0.00	0.00	0.00

Figure 14. Mode Shape MAC Values for FEA and SOS Results for Plate and Rib

REFERENCES

[1] Formenti, D. and Welaratna, S., "Structural Dynamics Modification--An Extension to Modal Analysis," SAE Paper Number 811043, 1980.

[2] Tayeb, M.M. and Williams, E.J., "Rib Stiffeners for Use in Structural Dynamics Modification," Proceedings of the 6th International Modal Analysis Conference, vol. 2, pp. 1094-1099, 1988.

[3] Structural Measurement Systems, Inc., "An Introduction to the Structural Dynamics Modification System," Technical Note Number 1, 1980.

[4] Wallack, P., Skoog, P. and Richardson, M., "Simultaneous Structural Dynamics Modification (S^2DM)," Proceedings of the 6th International Modal Analysis Conference, vol. 2, pp. 1033-1038, 1988.

[5] Allemang, R.J. and Brown, D.L., "A Correlation Coefficient for Modal Vector Analysis," Proceedings of the 1st International Modal Analysis Conference, pp. 110-116, 1982.